agronomy

MDPI

Article

The Clogging Rules of Ceramic Emitter in Irrigation Using Saline Water with Different EC

Huifang Chen [1], Yanfang Liu [2,*], Junying Chen [1,*], Lin Zhang [3], Yaohui Cai [1], Haiying Chen [4], Shoujun Wu [1] and Mingu Zhou [5]

1 College of Water Resources and Architectural Engineering, Key Laboratory of Agricultural Soil and Water Engineering in Arid and Semiarid Areas of Ministry of Education, Northwest A&F University, Yangling 712100, Shaanxi, China
2 College of Resources and Environmental Engineering, Ludong University, Yantai 264025, Shandong, China
3 Institute of Soil and Water Conservation, Northwest A&F University, Yangling 712100, Shaanxi, China
4 Department of Foreign Languages, Northwest A&F University, Yangling 712100, Shaanxi, China
5 Institute of Water Saving Agriculture in Arid Areas of China, Northwest A&F University, Yangling 712100, Shaanxi, China
* Correspondence: liuyanfang1988@126.com (Y.L.); cjyrose@126.com (J.C.); Tel.: +86-178-5457-9087 (Y.L.); +86-153-3926-8868 (J.C.)

Received: 25 June 2019; Accepted: 6 August 2019; Published: 8 August 2019



Abstract: Infiltration irrigation with saline water is a more effective method than drip irrigation to alleviate water scarcity worldwide, but so far, no report has discussed the clogging rules of ceramic emitters, a major component of infiltration irrigation system. To explore the clogging mechanism of ceramic emitter in saline water infiltration irrigation system, we used four kinds of saline water sources with electrical conductivity (EC) of 0.18, 1.74, 3.78, and 7.74 ds/m, respectively. In addition, we specifically investigated the law of discharge ratio variation (Dra) of ceramic emitters, as well as the composition and growth process of clogging substance. The results indicated that the Dra of ceramic emitters decreased in the process of saline water irrigation, and the higher the EC, the more obvious the decrease. The calcium carbonate ($CaCO_3$) was the main component of the clogging substance in the inner wall of ceramic emitters. The clogging part was a layer on the inner wall of the emitters rather than the pores in the walls, and the clogging did not occur suddenly. Instead, it was caused by the long–term accumulation of the clogging substance. Moreover, with the increase of EC, the flocculation between the clogging particles in the water was enhanced and thus promoted the formation of stable and compact aggregates, which fundamentally led to the clogging acceleration of ceramic emitters. This clogging mechanism of ceramic emitters can provide some theoretical reference for the establishment of anti-clogging strategy.

Keywords: infiltration irrigation; ceramic emitter; saline water; Dra; clogging substance; clogging part

1. Introduction

Saline water drip irrigation is a feasible method in areas where water is scarce or water competition is intense [1–3]. However, plastic water-saving products for drip irrigation such as emitters, pipes, and filters seriously restrict the popularization of drip irrigation technology because of the problems of high energy consumption, poor durability, and environmental pollution after aging [4–6]. Therefore, it is particularly important to seek a new irrigation technology that can meet the demands of large-scale field irrigation and produce good economic and ecological benefits. For this end, the Institute of Water-saving Agriculture in Arid Areas of China, Northwest A&F University developed a microporous ceramic emitter, which allows automatic irrigation and is both energy-efficient and environment-friendly [7]. The recombination of salt easily occurs during transport, and therefore, chemical clogging in saline

water irrigation [8]. When used in saline water irrigation, the ceramic emitters will be subject to clogging. Previous studies have indicated that the drip irrigation emitter clogging using saline water was closely related to the formation and agglomeration of chemical precipitation [9–11]. Hills et al. conducted drip irrigation experiment using saline water with electrical conductivity (EC) of 0.59, 1.12, and 2.02 ds/m, respectively, and found that the respective flow reductions for 50% of the tested emitters were 10%, 18%, and 29% [9]. Liu et al. found that the higher salt content the irrigation water had, the more intense the emitter clogging was, and that $CaCO_3$ was the main reason for the clogging [12]. Zhangzhong et al. discovered that the clogging of saline water irrigation system was an evolutionary process, and the formation and agglomeration of chemical precipitation (the major substance was calcium carbonate ($CaCO_3$)) in the system were the main reasons for emitter clogging. Besides, the higher pH, temperature, ion contents, and EC also promoted the formation of chemical precipitation, which resulted in serious emitter clogging [13]. Zhangzhong et al. studied the mechanism of emitters' chemical clogging in saline water drip irrigation and found that chemical precipitation adhered to the flow path of emitters, and that eventually, the cross-sectional area of the flow was reduced, which led to emitter clogging [14].

Thus far, scholars have made some achievements in emitter clogging research. However, most of these achievements are partial to the chemical clogging of emitters in saline water drip irrigation system, and the clogging of ceramic emitters in saline water infiltration irrigation system has not been reported yet. In addition, the complexity of saline water quality can easily lead to the formation of chemical precipitation, and chemical precipitation is liable to the pH, temperature, and ion contents [15–17], which makes the clogging process and mechanism of saline water infiltration irrigation system more complex. The increasingly wide application of saline water posed more challenge to the anti-clogging ability of ceramic emitter. Therefore, it is urgent to research the chemical clogging mechanism of ceramic emitters in infiltration system.

Therefore, we studied the effects of the saline water with different EC on ceramic emitter clogging and chemical precipitation formation, analyzed its inducing mechanism, identified the chemical characteristics of the clogging substance, and explored the clogging mechanism of ceramic emitter. The results could provide theoretical reference for the control scheme formulation of saline water infiltration irrigation system and the extension of ceramic emitters.

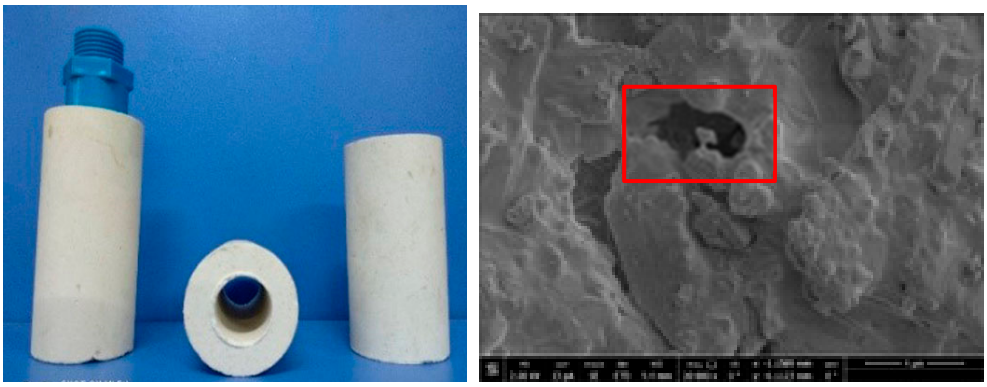
2. Materials and Methods

2.1. Micrporous Ceramic Emitters

The microporous ceramic emitter in the experiment was developed by China's Northwest A&F University. The ceramic emitter is a new type of underground irrigation emitter. It has a fixed ratio of raw material and a systematic preparation process. Its major parameters are shown in Table 1. The working principle of ceramic emitters consisted of infiltration of the irrigation water into crop root soil through interconnected emitter pores. Its process consisted of penetration of the irrigation water through the inner wall to the outer wall, and infiltration into the surrounding soil through the outer wall of the ceramic emitter. Its overall structure is shown in Figure 1a, and the pores in the wall observed by scanning electron microscope (SEM) (4 μm at × 20,000) are shown in Figure 1b.

Table 1. Major parameters of ceramic emitter.

Outside Diameter (cm)	Inside Diameter (cm)	Height (cm)	Design Discharge (L/h)
4.0	2.0	8.0	0.07



(**a**) (**b**)

Figure 1. The construction of ceramic emitter (**a**), the pores in the wall of unused ceramic emitter observed by SEM (**b**).

2.2. Water Source

In general, saline water is water with salinity of 2~5 g/L. With reference to the saline water quality in Mosuowan irrigation area of Xinjiang, we prepared saline water with salinity of 1, 3, and 6 g/L, respectively. Specifically, we added $NaHCO_3$, Na_2SO_4, NaCl, and $CaCl_2$ at the mass ratio of 1:7:8:2 into Yangling groundwater (EC = 0.18 ds/m). The EC of the four types of treated saline water (recorded as W0, W1, W2, and W3) are 0.18, 1.74, 3.78, and 7.74 ds/m, respectively. The contents of Ca^{2+} and Na+ were determined by the Atomic Absorption Spectrometry; the SO_4^{2-} by the Barium Chromate Spectrophotometry; the HCO_3^- and CQ_3^{2-} by the hydrochloric Acid Titration; the Cl^- by the Silver Nitrate Titration; the hardness by the EDTA method; the total dissolved solids and suspended solids by the weighing method; the pH by the glass electrode method; and EC by the conductivity meter method. The major water quality parameters of the four irrigation water sources are shown in Table 2.

Table 2. Water quality parameters of four irrigation water sources.

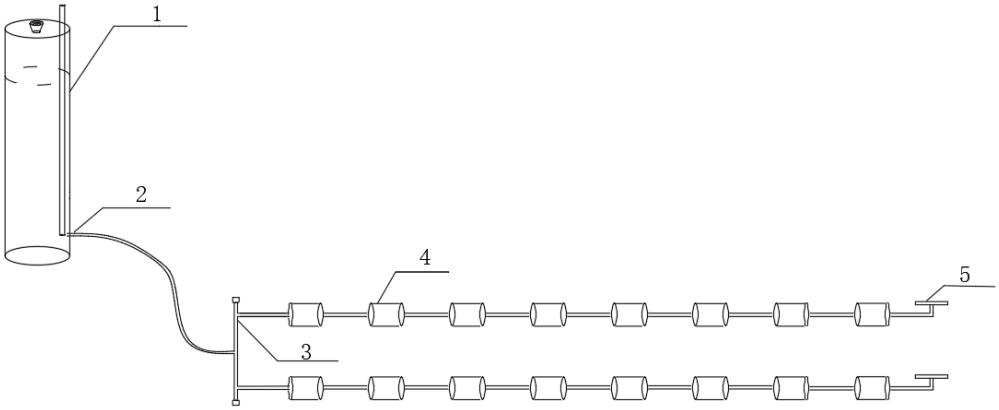
	Ion Contents ($mg \cdot L^{-1}$)						Hardness	pH	Dissolved Solids	Suspended Solids	EC
Treatment	Ca^{2+}	Na^+	SO_4^{2-}	HCO_3^-	Cl^-	CQ_3^{2-}	$mg \cdot L^{-1}$		$mg \cdot L^{-1}$	$mg \cdot L^{-1}$	$ds \cdot m^{-1}$
W0	29	5	47.2	86.1	7	0	92.08	6.80	105	0	0.18
W1	78	333	332	132.86	335	0	198.18	7.62	1116	0	1.74
W2	191	1066.70	860	205.32	1020	0	369.33	7.58	3128	0	3.78
W3	338	2092.70	1637	283.20	2015	0	611.55	7.56	6015	0	7.74

2.3. Experimental Design

The infiltration irrigation testing chamber was built in the Irrigation Hydraulic Laboratory, the Institute of Water-saving Agriculture in Arid Areas of China, Northwest A&F University. Four independent infiltration irrigation test systems were arranged according to four kinds of water sources, and each test chamber is illustrated in Figure 2. For each test, the Mariotte bottle (20 × 100 cm, diameter × height) was used as a water supply device and two parallel arranged laterals with eight ceramic emitters were installed. The emitters were connected with PVC pipes (inside diameter was 20 mm) and the spacing was 15 cm. The experiment adopted the continuous irrigation method, and was conducted from May 28 through August 16, 2018. The test lasted 81 days. Irrigation water was regularly replenished in Mariotte bottles throughout the test and the infiltration irrigation system was not flushed during the whole test.



(**a**) Testing device.



1 - Mariotte bottle, **2** - water pipe, **3** - PVC pipe, **4** - ceramic emitter, **5** - water valve

(**b**) Scheme of the main emitter treatment system

Figure 2. Layout of the testing chamber.

2.4. Test Content and Methods

2.4.1. Water Temperature Monitoring

The saline water temperature was monitored using mercurial thermometer (minimum scale: 0.5 °C) at 9:00, 12:00, 15:00, and 18:00 every day, and the average value was taken as the water temperature of the day. The average temperature during the test is shown in Figure 3. The average water temperature varied with the change of the weather during the test period, and the highest and lowest water temperatures were 34.00 °C and 18.25 °C, respectively.

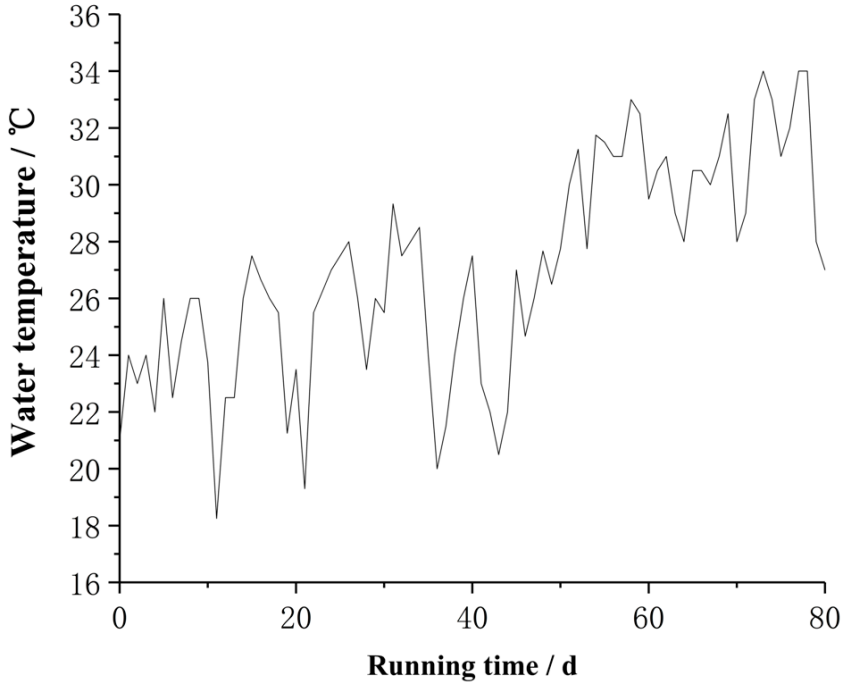


Figure 3. Variation of irrigation water temperature.

2.4.2. The Discharge Test of Ceramic Emitter

The discharge of the ceramic emitter was measured at 9:00, 12:00, 15:00, and 18:00 every day, and the average value was taken as emitter discharge of the day. When the discharge was measured, measure cups with a volume of 1 L were placed successively below each emitter every 5 s to collect the discharge. The cups were rapidly removed from the testing emitters after the flow had been collected for 20 min. The weight of measuring cup was measured with an electronic balance (accuracy: 0.01 g) before the measurement of the emitter discharge. Then, the related data were recorded.

2.4.3. Clogging Substance Analysis

To verify the continuous change of the clogging substance in the emitter during the test, the emitter was sampled regularly during the irrigation process. An emitter was taken down from each irrigation system after running for nine days and connected with a PVC pipe at the same site. To ensure that the emitter discharge was not affected by sampling, we sampled only twice during the test process. The final sample was taken at the end of the irrigation. Emitter samples was taken three times, and the sampling dates were the 10th, 19th, and 81th day, respectively. Samples were dried in the oven at the temperature of 80 °C. The dried emitter was vertically divided into two parts. One part was used to collect clogging substance from the inner wall of ceramic emitter and the other was used to make SEM observation samples.

Composition analysis of the clogging substance: the clogging substance attached to the inner wall of ceramic emitter was scanned by the X-ray diffraction (XRD), and the obtained polycrystalline diffraction image was qualitatively analyzed using the analysis software (Jade 6) to determine the composition of the clogging substance.

Sample image acquisition and clogging composition analysis: The samples were made into observation samples. The structure of the clogging substance attached to the inner wall and the pores in the wall of the ceramic emitter was observed with the SEM. Multiple photos of the clogging substance were taken continuously during the observation process, and the clogging substance shown in the image was subjected to Energy spectrum analysis to determine its constituents. The observation area of ceramic emitter under SEM is the marked part shown in Figure 4. Each sample has two observation

locations. One is the inner wall of the ceramic emitter (A), the other is the pores in the wall of the ceramic emitter (B).

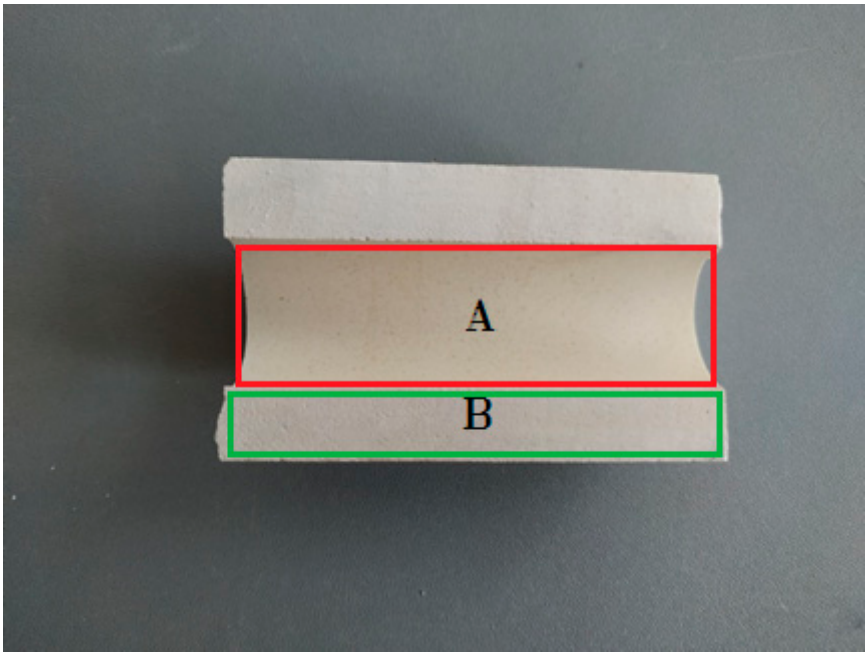


Figure 4. The observation locations of the ceramic emitter.

2.5. Drip Irrigation System Performance Evaluation Index

The emitter discharge is mainly related to the type of the emitter, working pressure, and water temperature. In this study, we guaranteed these influence factors consistently under four treatments. Variations in Dra were determined to evaluate the flow, which reflected the emitter clogging levels. It directly reflected the reduction in flow rates of the emitters. The value was calculated based on the measured flow rates. The Dra of the ceramic emitters in each treatment was calculated with Equation (1):

$$D_{ra} = \frac{1}{n}\sum_{i=1}^{n}(q_i/q_0) \times 100\ [\%] \quad (1)$$

In Equation (1), q_i is the average discharge of the tested ceramic emitter, in L/h; q_0 represents the initial discharge of ceramic emitter tested, in L/h; n stands for the total number of tested ceramic emitters in each treatment, n is 16.

2.6. Statistical Analysis Method

The experimental data were organized using Excel, and all the Dra data were the average values of each replicate. The Fourier analysis tool was used to design smooth curves through each Dra point set. The statistical software SPSS 23 was used to analyze the significance analysis of Dra, and Origin 2016 was used to draw the XRD date chart.

3. Results and Analysis

3.1. Effects of Saline Water with Different EC on the Discharge Rate of Ceramic Emitter

Figure 5 shows the dynamic variation of the ceramic emitter Dra in four treatments. Table 3 shows the significant analysis of Dra under the four treatments. As shown in Figure 5, in the initial stage of experiment, the pressure of water supply system was disturbed by sampling, which led to the wide fluctuations in the emitter discharge. Meanwhile, it was found that the emitter discharge also

fluctuated every day after eliminating the effect caused by sampling on emitter discharge. Comparison of the fitted curves for running time to the Dra of emitter under the four treatments in Figure 5, the Dra of W0 changed very little while the system operated, however, the emitter Dra of W1, W2, and W3 decreased. Besides, with the increase of EC, the more severe of the emitter Dra downtrend the higher of degree of clogging. This indicated that the emitter discharge rate was related to the irrigation duration and the levels of salt in irrigation water.

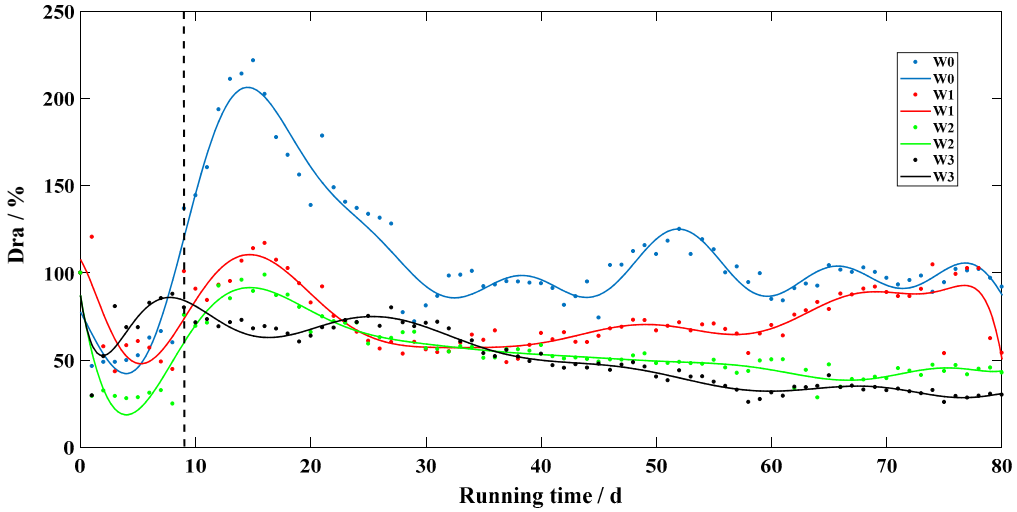


Figure 5. Variations of emitter Dra with different saline water. The sampling time (the date is the 10th d) is indicated by a dotted line.

Table 3. Significance analysis of Dra under the four treatments.

	W0	W1	W2	W3
W0	1	0.563 **	0.823 **	0.272 *
W1	-	1	0.426 **	−0.105N
W2	-	-	1	0.511 **
W3	-	-	-	1

Note: In the table, N means not significant, * means significant ($p < 0.05$), ** means extremely significant ($p < 0.01$).

According to the clogging standard by the international organization for standardization, it is believed that the clogging begins when the actual flow rate of the emitter drops to 75% of the rated flow rate [18]. According to Figure 5, at the end of the test, the Dra of the four treatments were reduced to 91.95%, 54.05%, 42.68%, and 30.00% of the initial flow, respectively. In comparison, the Dra of W1, W2, and W3 were 37.90%, 49.27%, and 61.95% lower than that of W0, respectively. As shown in Table 3, the difference in Dra between W0 and W3 reached a significant level, while that among W0, W1, and W2 were extremely significantly different from each other. It can be concluded that the discharge decreases of W1, W2, and W3 are significantly greater than that of W0.

In addition, the W0 and W1 Dra's displayed a sharp decrease at the end of the test. The reason for this phenomenon was that the Dra of W0 and W1 had a small value at the end of the test and the fitting process of curves matched as many scattered points as possible, which caused a sharp decrease of the fitted curves. Besides, the appearance of local peak was a common phenomenon in the fitting process, and it did not mean that the future trend was a steep rise or fall.

3.2. Composition Analysis of the Clogging Substance

The results of XRD scanning of the clogging substance were shown in Figure 6. The polycrystalline diffraction peaks of the sample were intricate, which indicated that the sample composition was very complex. Considering that there may be adhesion between the inner wall of the ceramic emitter and

the clogging substance, it was possible that the adhesive substance might contain the components of the ceramic emitter when the clogging substance was extracted from the inner wall of the ceramic emitter. Compared with the unused emitter, it can be seen that the composition of the clogging substance was preliminarily determined by $CaCO_3$, quartz (SiO_2), silicate ($CaAl_2Si_2O_84H_2O$), and so forth. To determine the exact composition of the clogging substance, further analysis should be conducted to the inner wall of the ceramic emitter.

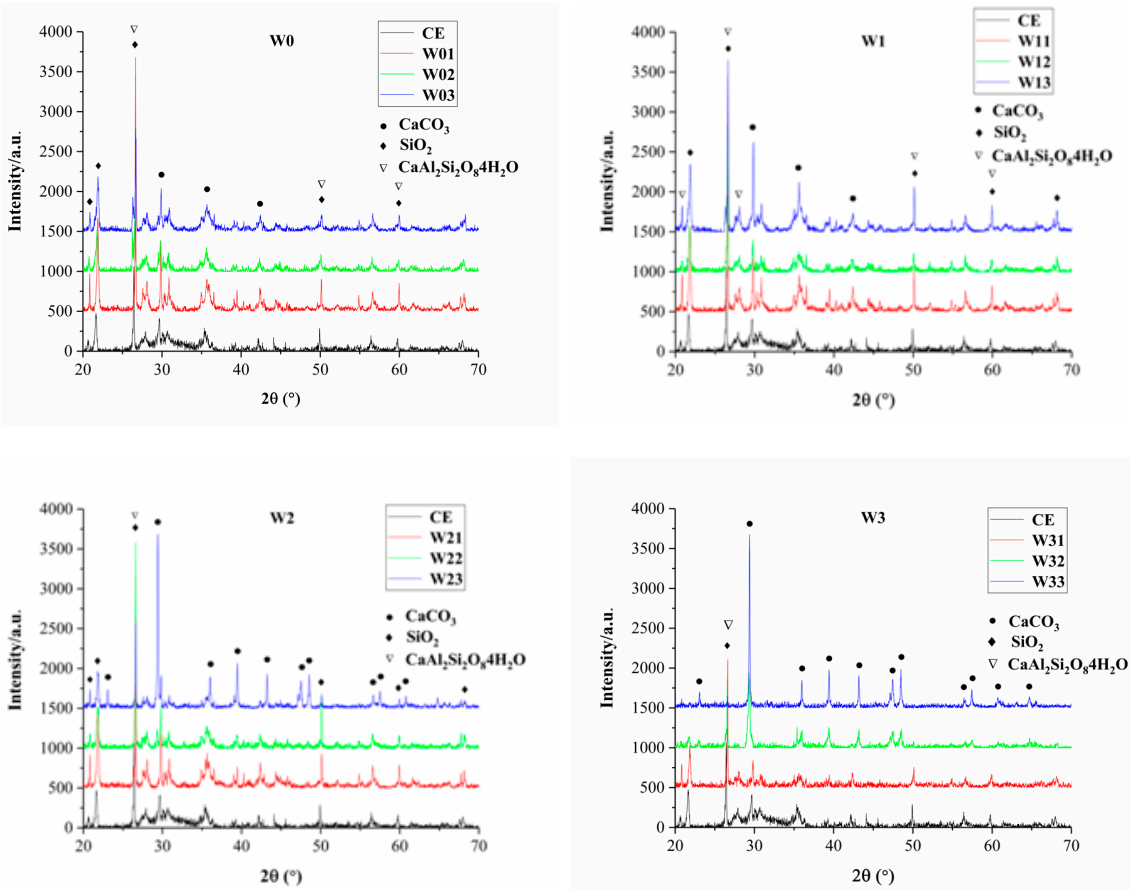


Figure 6. The clogging substance analyzed with XRD. The mountain like curve is XRD pattern we detect from the X-ray Diffractometer, x axis is 2θ/degree and the y axis represent the intensity. We can read the chemistry constituents of clogging substance. CE is the component of ceramic emitter, and 1, 2, 3 in W01, W02, W03 represent samples taken on 10th d, 19th d, and 81th d under W0 treatment. W1, W2, and W3 are the same as W0.

Table 4 was the mass percentage of each major element in the clogging substance in the inner wall of the ceramic emitter at the end of the test obtained through the Energy spectrum analysis. The chemical elements were consistent under the four treatments, including C, O, Ca, Si, Cl, Na, and Al. The most abundant elements were C, O, and Ca. Considering the large amount of Ca^{2+} and HCO_3^- in each treatment, it can be speculated from the element content that Ca^{2+} and HCO_3^- in irrigation saline water would react to form $CaCO_3$. Meanwhile, the clogging substance contained little Cl and Na. The soluble sodium salts could have been present because sodium chloride (NaCl) was wrapped in the clogging substance during the chemical clogging formation [13].

Table 4. Mass percentage analysis of each element of the clogging substance.

Treatments	C	O	Ca	Si	Cl	Na	Al	Total
W0	19.91	40.51	36.21	0.78	0.71	1.41	0.48	100.01
W1	16.73	46.69	31.76	1.92	0.90	1.19	0.81	100
W2	15.71	57.78	25.81	0.06	0.05	0.54	0.04	99.9
W3	20.53	49.89	24.86	0.41	1.69	1.76	0.86	100

By comprehensive analysis of Figure 6 and Table 4, it can be concluded that the composition of clogging substance in the ceramic emitter consists of $CaCO_3$, SiO_2, $CaAl_2Si_2O_84H_2O$, and a little NaCl, among which $CaCO_3$ accounts for the largest proportion.

3.3. Image Analysis of Clogging Substance Structure in Ceramic Emitter

The microstructure of inner wall clogging substance and the pores in the wall of ceramic emitter observed by SEM (4 μm at × 20,000) are shown in Figures 7 and 8, respectively. As shown in Figure 7, the clogging substance had a rough surface and complex structure. It was clearly seen that the substance was composed of crystal particles inconsistently. Its compactness and surface structure complexity increased over the running time. Its structure varied from one EC to another. As marked in Figure 7, under the treatment of W0, the area of a single particle was about 10 μm^2, the flocculation between particles in the emitter was not obvious, and it was difficult to form a large stable accumulation body. The crystal particles forming the accumulation body were relatively small and mainly existed dispersedly. The surface of the clogging substance was relatively smooth. The area of a single particle was about 13 μm^2 under the treatment of W1. Compared with W0, the flocculation between the clogging particles enhanced and the crystal particles forming the accumulation body were relatively dense. When under the treatment of W2, the area of a single particle was about 19 μm^2, and when under the treatment of W3, the area was about 27 μm^2. Compared with W0 and W1, the flocculation of clogging particles, as well as the density and surface structure complexity, under the treatment of W2 and W3 was significantly enhanced. In addition, the clogging substance was lumpy compact accumulation body. In general, with the increasing of the EC, the size and tightness of the clogging particles were increased. Thus, the risk of accelerating the emitter clogging became greater during the procedure.

As marked in Figure 8, compared with the ceramic emitter before its use, no clogging crystal particles were found in the pores of the experimental ceramic emitter. Therefore, it can be concluded that the pores in the walls were not the clogging parts of the emitter.

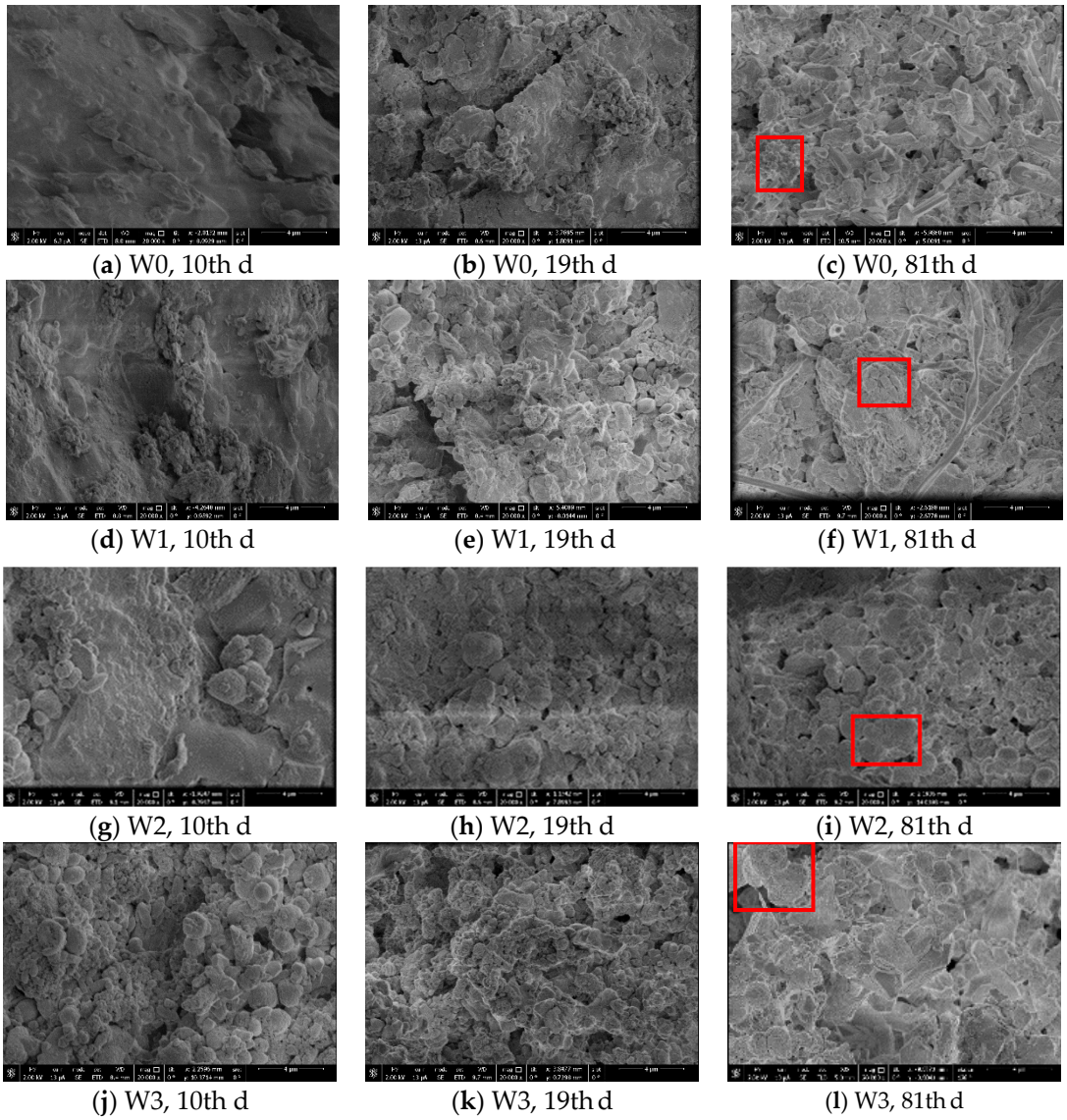
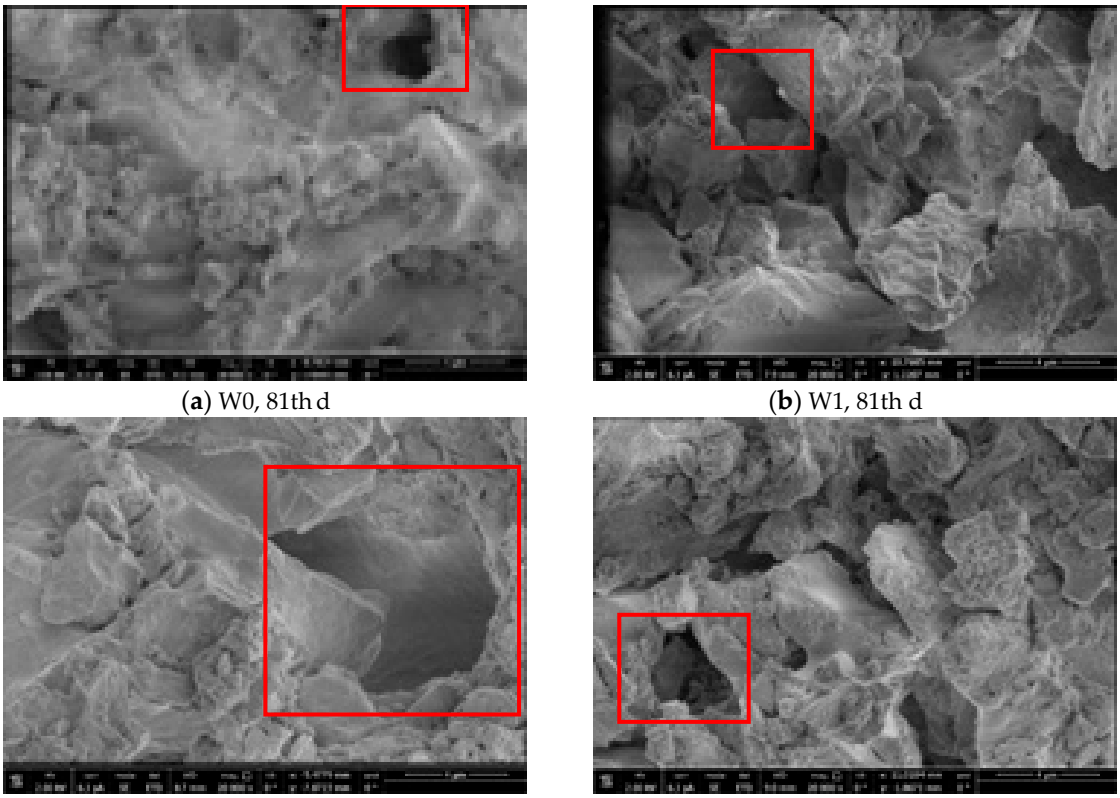


Figure 7. The inner wall clogging substance of ceramic emitter observed by SEM. (**a**) The sampling time at the 10th d, W0, 4 μm at ×20,000; (**b**) the sampling time at 19th d, W0, 4 μm at ×20,000; (**c**) the sampling time at 81th d, W0, 4 μm at ×20,000; (**d**) the sampling time at 10th d, W1, 4 μm at ×20,000; (**e**) the sampling time at 19th d, W1, 4 μm at ×20,000; (**f**) the sampling time at 81th d, W1, 4 μm at ×20,000; (**g**) the sampling time at 10th d, W2, 4 μm at ×20,000; (**h**) the sampling time at 19th d, W2, 4 μm at ×20,000; (**i**) the sampling time at 81th d, W2, 4 μm at ×20,000; (**j**) the sampling time at 10th d, W3, 4 μm at ×20,000; (**k**) the sampling time at 19th d, W3, 4 μm at ×20,000; (**l**) the sampling time at 81th d, W3, 4 μm at ×20,000. We can obtain the microstructure of inner wall clogging substance in the images.



(**a**) W0, 81th d (**b**) W1, 81th d

(**c**) W2, 81th d (**d**) W3, 81th d

Figure 8. The pores in the wall of ceramic emitter observed by SEM. (**a**) the sampling time at 81th d, W0, 4 μm at ×20,000; (**b**) the sampling time at 81th d, W1, 4 μm at ×20,000; (**c**) the sampling time at 81th d, W2, 4 μm at ×20,000; (**d**) the sampling time at 81th d, W3, 4 μm at ×20,000. We can obtain the microstructure of the pores in the wall in the images.

4. Discussion

Through the experiment of saline water infiltration irrigation, it is found that the Dra of the ceramic emitter decreased in the irrigation process. Comparison of the emitter Dra under the four treatments found the Dra of ceramic emitter decreased with the increase of EC. The reason for this phenomenon is that the concentration of various ions (Ca^{2+}, HCO_3^-, etc.) increased with the rise of the EC, and the risk of the emitter clogging was thus enhanced. In terms of the emitter, discharge fluctuated under saline water irrigation. The reason for this phenomenon is unknown. Therefore, further research may focus on the emitter discharge fluctuated in infiltration irrigation.

To clarify the characteristics of the clogging substance inside the ceramic emitter is the premise and foundation of exploring the clogging mechanism and establishing the effective control measures. Relevant studies have shown that the main chemical clogging substance in the drip irrigation emitter were calcium or magnesium carbonate, calcium sulfate, heavy metal hydroxides, oxides, carbonates, silicates, sulfides, and fertilizers (phosphate, aqueous ammonia, iron, zinc, copper, and manganese) [19]. In the present study, chemical clogging of ceramic emitter under the saline water quality in Mosuowan irrigation area of Xinjiang was analyzed, and the results revealed that the compositions of the clogging substance in the ceramic emitters were $CaCO_3$, SiO_2, $CaAl_2Si_2O_84H_2O$, and a little NaCl. The saline water in this experiment contained a large quantity of SO_4^{2-}, but no $CaSO_4$ was found in the clogging substance because the $CaCO_3$ is less soluble than that of $CaSO_4$, which resulted in no $CaSO_4$ in the clogging substance.

The irrigation water parameters play a critical role in the formation of chemical precipitation, but the water EC, pH, and temperature are the key factors affecting the emitter clogging. Previous investigations have indicated that the degree of emitter clogging also grew with the increase of

suspended particles, EC, and ion concentration of calcium and magnesium. Serious emitter clogging could occur when the irrigation water EC was higher than 4.5 ds/m [15,20]. This study indicated that the experimental saline water with higher EC could easily form chemical precipitates, leading to the different levels of emitter clogging. Additionally, with the rise of the EC, the concentration of various ions increased, which promoted the formation and agglomeration of chemical precipitation. Nakayama and Bucks found when pH < 7.0, the chemical precipitation may lead to mild emitter clogging; when 7.0 < pH < 8.0, moderate clogging; and when pH > 8.0, severe clogging [21]. In the present study, the respective pH values of saline water of W1, W2, and W3 were 7.62, 7.58, and 7.56, which were all above 7, and provided a favorable environment for the formation of $CaCO_3$ and easily caused moderate emitter clogging. For irrigation water with W0 (EC is 0.18 ds/m), the pH value, although in the range of mild clogging, was close to the lower limit of the moderate clogging range, so it might have a certain effect on the clogging. These findings are in accordance with previous studies of the emitter clogging performance [22]. Although the temperature variation cannot directly lead to the clogging, it can accelerate the deposition of chemical sediments and induce the emitter clogging. Hills et al. studied the effect of temperature on chemical clogging and found that with the increase of the temperature, the deposition of calcium carbonate was promoted and the clogging was aggravated [9]. In the process of this experiment, the saline water temperature fluctuated within the range of 18.25 °C–34.00 °C, putting infiltrating irrigation system in a high-temperature environment. To a certain extent, it also aggravated the chemical precipitation and increased the clogging degree. The fundamental reason is that $CaCO_3$ has anomalous solubility, and the increase of temperature reduces its solubility.

The clogging occurred in the inner wall but not in the pores in the wall of the ceramic emitter. Based on the composition of the clogging substance and the distribution features (Figures 6 and 8), the clogging process was as follows (Figure 7): Chemical precipitation entered the emitter with irrigation water and then randomly adhered to its inner wall to form a adhesion layer. As the system operated, chemical precipitation flowed into the emitter continuously, making the inner wall increasingly rough. The chemical precipitation grew and agglomerated more easily in the inner wall, resulting in an increasingly thick adhesive layer and gradually forming sediments that clogged the inner wall. In terms of the clogging mechanism, this process commonly contributes to the emitter clogging. It can be concluded that the clogging was not caused by a sudden formation. Instead, the clogging substance accumulated over a long period of time.

In addition, the clogging part was the inner wall rather than the pores of the ceramic emitter, so we can take effective measures to restrict the formation of attached chemical precipitation, such as filtering out particles from the irrigation water, lateral flushing, material modification, and emitter structure optimization. Thus, further experiments and analysis should be conducted to explore the strategies of controlling clogging. This study can provide reference for the establishment of anti-clogging strategy after the application of the ceramic emitter.

It has been found that the clogging of drip irrigation emitter begins with biological enrichment, and the microbial biofilm and the extracellular polymer secreted by microorganisms will adsorb solid particles and organic matter to form large aggregates and induce emitter clogging [23–26]. In this experiment, the temperature was appropriate, and the environment was humid in the ceramic emitter. The saline water provided necessary nutrients, such as Na^+ and Ca^{2+} for microorganisms, so there was a relatively high possibility of biofilm formation in the emitter in the irrigation process. Therefore, further research may focus on the biofilm formation in infiltration irrigation.

5. Conclusions

In this study, we conducted an in-depth investigation into the chemical clogging mechanism of ceramic emitter in saline water infiltration irrigation and focused on the Dra variation. Specifically, we explored the composition and the dynamic formation process of the clogging substance in the ceramic emitter. Four conclusions were drawn as follows.

First, the application of saline water irrigation will indeed lead to a decrease in the discharge rate of the emitter, and the high EC has an obvious accelerating effect on the ceramic emitter clogging. Within a certain range, the accelerating effect of the emitter clogging is more obvious with the increase of the EC.

Second, the clogging substance attached to the inner wall of the ceramic emitters contained $CaCO_3$, SiO_2, $CaAl_2Si_2O_84H_2O$, and a little NaCl, among which the $CaCO_3$ was the primary substance that induced the emitter clogging.

Third, the clogging part was the inner wall rather than the pores of the ceramic emitter. It was found that emitter clogging was a progressive process rather than an abrupt event.

Fourth, as the EC of saline water increased, the chance of collision between the particles of the clogging substance grew and thus promoted the formation of a stable clogging deposit, which was the fundamental cause of accelerated clogging.

Author Contributions: J.C. and Y.L. conceived and designed the experiments, authored or reviewed drafts of the paper, approved the final draft; H.C. performed the experiments, analyzed the data, prepared figures and tables and wrote the paper; L.Z., Y.C., S.W. and M.Z. contributed materials/analysis tools; H.C. reviewed the paper.

Funding: This research was funded by the National Key Research and Development Program of China, grant number 2017YFC0403302; Humanities and Social Science Program of Northwest A&F University, grant number Z109021405; and the National Natural Science Fund of China, grant number 51879225.

Conflicts of Interest: The authors declare no conflict of interest.

References

1. Patel, R.M.; Prasher, S.O.; Donnelly, D. Subirrigation with brackish water for vegetable production in arid regions. *Bioresour. Technol.* **1999**, *70*, 33–37. [CrossRef]
2. Selim, T.; Berndtsson, R.; Persson, M. Simulation of soil water and salinity distribution under surface drip irrigation. *Irrig. Drain.* **2013**, *62*, 352–362. [CrossRef]
3. Lei, T.W.; Xiao, J.; Li, G.Y. Effect of drip irrigation with saline water on water use efficiency and quality of watermelons. *Water Resour. Manag.* **2003**, *17*, 395–408. [CrossRef]
4. Pei, Y.T.; Li, Y.K.; Liu, Y.Z. Eight emitters clogging characteristics and its suitability under on-site reclaimed water drip irrigation. *Irrig. Sci.* **2014**, *32*, 141–157. [CrossRef]
5. Capra, A.; Scicolone, B. Emitter and filter tests for wastewater reuse by drip irrigation. *Agric. Water Manag.* **2004**, *68*, 135–149. [CrossRef]
6. Li, G.B.; Li, Y.K.; Xu, T.W. Effects of average velocity on the growth and surface topography of biofilms attached to the reclaimed wastewater drip irrigation system laterals. *Irrig. Sci.* **2012**, *30*, 103–113. [CrossRef]
7. Cai, Y.H.; Wu, P.T.; Zhang, L. Simulation of infiltration characteristics of porous ceramic emitter under non-pressure condition. *J. Hydraul. Eng.* **2017**, *48*, 730–737, (In Chinese with English abstract). [CrossRef]
8. Sahin, U.; Tunc, T.; Eroğlu, S. Evaluation of $CaCO_3$ clogging in emitters with magnetized saline waters. *Desalin. Water Treat.* **2012**, *40*, 168–173. [CrossRef]
9. Hills, D.J.; Nawar, F.M.; Waller, P.M. Effects of Chemical Clogging on Drip-Tape Irrigation Uniformity. *Trans. ASAE* **1989**, *32*, 1202–1206. [CrossRef]
10. Eroglu, S.; Sahin, U.; Tunc, T. Bacterial application increased the flow rate of $CaCO_3$-clogged emitters of drip irrigation system. *J. Environ. Manag.* **2012**, *98*, 37–42. [CrossRef]
11. Aali, K.A.; Liaghat, A.; Dehghanisanij, H. The effect of acidification and magnetic field on emitter clogging under saline water application. *J. Agric. Sci.* **2009**, *1*, 132–141. [CrossRef]
12. Liu, Y.F.; Wu, P.T.; Zhu, D.L. Effect of water hardness on emitter clogging of drip irrigation. *Trans. CSAE* **2015**, *31*, 95–100, (In Chinese with English abstract). [CrossRef]
13. Zhangzhong, L.L.; Yang, P.L.; Ren, S.M. Chemical clogging of emitters and evaluation of their suitability for saline water drip irrigation. *Irrig. Drain.* **2016**, *65*, 439–450. [CrossRef]
14. Zhangzhong, L.L. Mechanism of the Emitters Chemical-Clogging under Drip Irrigation with Saline Water and its Preventation Methods. Ph.D. Thesis, China Agricultural University, Beijing, China, 2016.
15. Capra, A.; Scicolone, B. Water quality and distribution uniformity in Drip/Trickle irrigation systems. *J. Agric. Eng. Res.* **1998**, *70*, 355–365. [CrossRef]

16. Yuan, Z.; Waller, P.M.; Choi, C.Y. Effects of organic acids on salt precipitation in drip emitters and soil. *Trans. ASAE* **1998**, *41*, 1689–1696. [CrossRef]
17. Sheta, A.S.; Al-Sewailem, M.S.; Sallam, A.S. Nature and Composition of Newly Formed Precipitates in Relationship to Characteristics of Groundwater in Arid Environment. *Arid Soil Res. Rehab.* **2000**, *14*, 387–401. [CrossRef]
18. *ISO/TC 23/SC 18/WG5 N4: Clogging Test Methods for Emitters*; International Organization for Standardization: Geneva, Switzerland, 2003.
19. Bucks, D.A.; Nakayama, F.S.; Gilbert, R.G. Trickle irrigation water quality and preventive maintenance. *Agric. Water Manag.* **1979**, *2*, 149–162. [CrossRef]
20. Shinde, D.G.; Patel, K.G.; Solia, B.M. Clogging behaviour of drippers of different discharge rates as influienced by different fertigation and irrigation water salinity levels. *J. Environ. Res. Dev.* **2012**, *7*, 917–922.
21. Nakayama, F.S.; Bucks, D.A. Water quality in drip/trickle irrigation: A review. *Irrig. Sci.* **1991**, *12*, 187–192. [CrossRef]
22. Dehghanisanij, H.; Yamamoto, T.; Rasiah, V. Impact of biological clogging agents on filter and emitter discharge characteristics of microirrigation systems. *Irrig. Drain.* **2004**, *53*, 363–373. [CrossRef]
23. Yan, D.Z.; Yang, P.L.; Li, Y.K. Evaluation of drip emitter clogging with reclaimed wastewater irrigation. *Trans. CSAE* **2011**, *27*, 19–24, (In Chinese with English abstract). [CrossRef]
24. Persyn, R.A.; Lesikar, B.J.; Duan, X.J. Uniformity of domestic wastewater effluent application in a subsurface drip distribution system. *Water Environ. Res.* **2007**, *79*, 701–706. [CrossRef] [PubMed]
25. Li, Y.K.; Liu, H.S.; Yang, P.L. Analysis of tracing ability of different sized particles in drip irrigation emitters with computational fluid dynamics. *Irrig. Drain.* **2013**, *62*, 340–351. [CrossRef]
26. Ahmed, B.A.O.; Yamamoto, T.; Fujiyama, H. Assessment of emitter discharge in microirrigation system as affected by polluted water. *Irrig. Drain.* **2007**, *21*, 97–107. [CrossRef]



© 2019 by the authors. Licensee MDPI, Basel, Switzerland. This article is an open access article distributed under the terms and conditions of the Creative Commons Attribution (CC BY) license (http://creativecommons.org/licenses/by/4.0/).